nature physics

SUPPLEMENTARY INFORMATION

https://doi.org/10.1038/s41567-018-0408-1

In the format provided by the authors and unedited.

Terahertz-driven phonon upconversion in $SrTiO_3$

M. Kozina[1*], M. Fechner[2], P. Marsik[3], T. van Driel[1], J. M. Glownia[1], C. Bernhard[3], M. Radovic[4], D. Zhu[1], S. Bonetti[5], U. Staub[4] and M. C. Hoffmann[1]

[1]Linac Coherent Light Source, SLAC National Accelerator Laboratory, Menlo Park, CA, USA. [2]Max Planck Institute for the Structure and Dynamics of Matter, Hamburg, Germany. [3]Department of Physics, University of Fribourg, Fribourg, Switzerland. [4]Swiss Light Source, Paul Scherrer Institut, Villigen, Switzerland. [5]Department of Physics, Stockholm University, Stockholm, Sweden. *e-mail: mkozina@stanford.edu

Supplementary Information

Kozina et al, "Terahertz-Driven Phonon Upconversion in $SrTiO_3$"

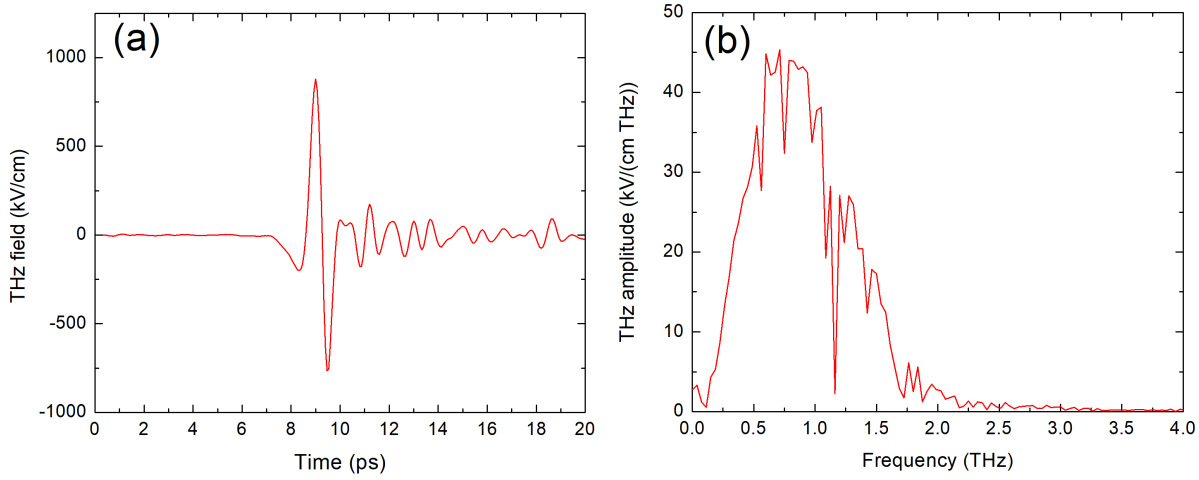

Figure S1 Terahertz pump waveform: ***a*** *Electro-optic sampling signal of terahertz (THz) pump at sample location measured in-situ by electro-optic sampling in a 50 µm thick (110) GaP crystal.* ***b*** *Magnitude of frequency spectrum of the THz waveform in* ***a*** *calculated by Fast Fourier Transform. The intensity was adjusted with wiregrid polarizers (Infraspecs P01) without changing the THz waveform.*

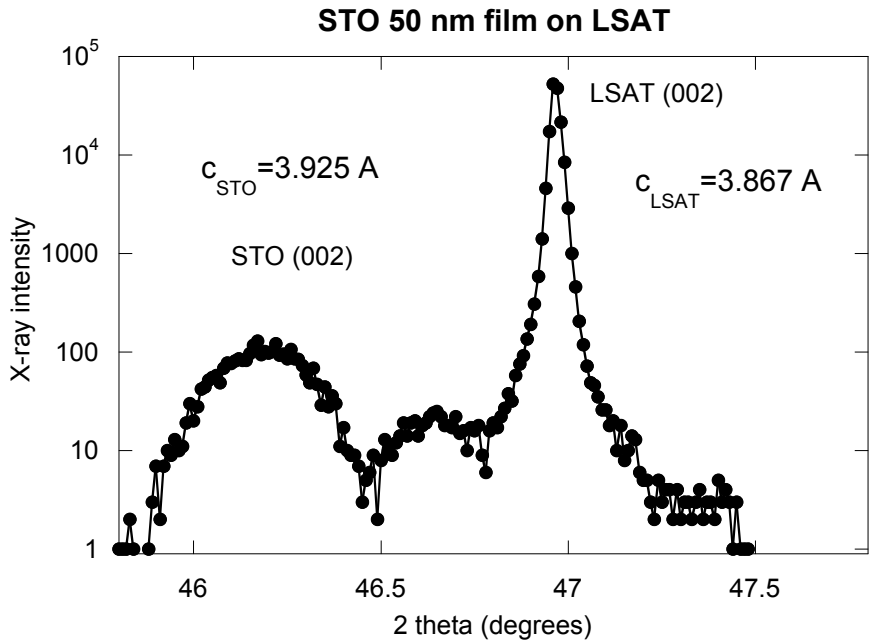

Figure S2: Two-Theta scan of sample before annealing*. Static x-ray diffraction pattern along sample normal. The low-angle peak corresponds to the STO film and the sharp peak at higher angle is the LSAT substrate. We observe clear splitting along the cross-plane direction between the substrate and the film. These measurements were taken before the sample was annealed.*

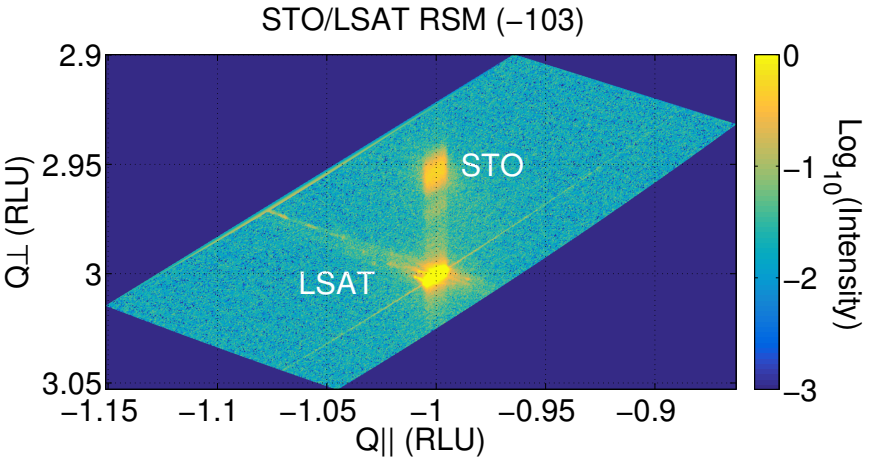

Figure S3: Reciprocal space map of the sample before annealing. *Static reciprocal space map collected on a similar sample prior to annealing about the (-1 0 3) reciprocal lattice point using a Cu kα source. The separation between the film and substrate peaks along the cross-plane direction shows there is a difference in lattice parameter, whereas there is clear indication that in-plane the film and substrate are lattice matched to the LSAT unit cell.*

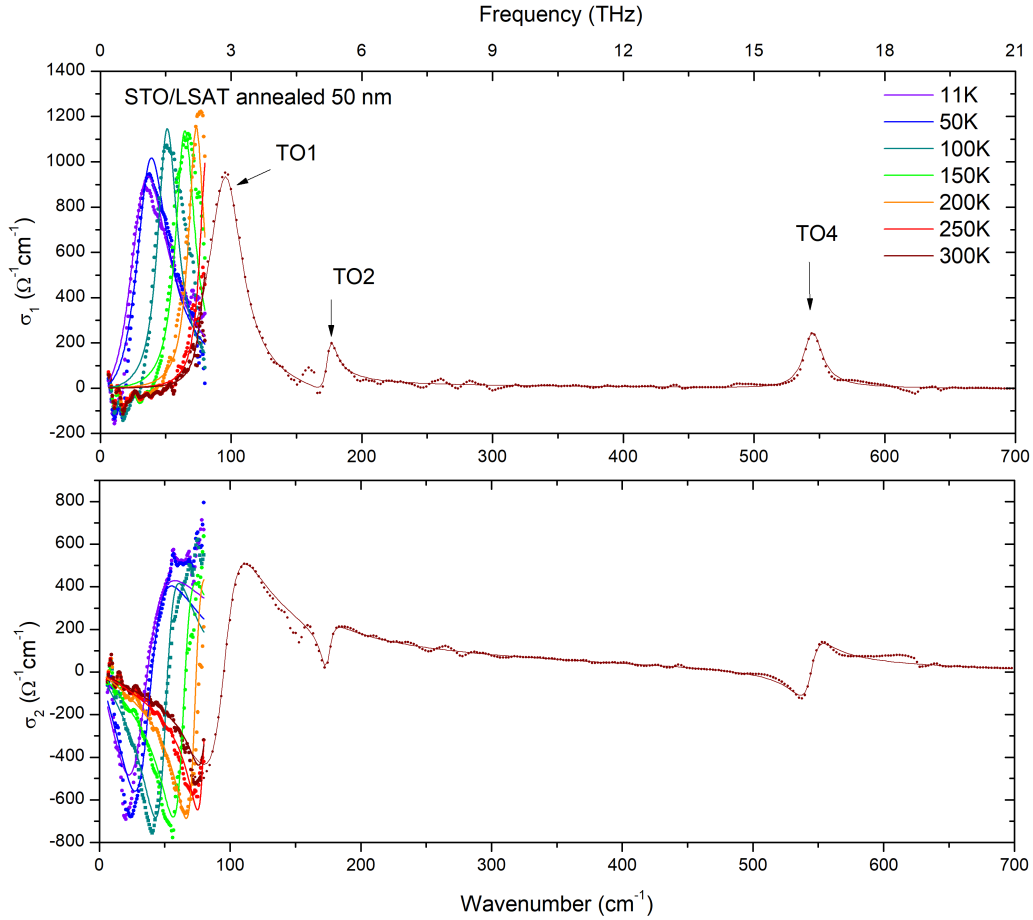

Figure S4: Optical conductivity of the annealed sample. *We show additional ellipsometry measurements on our sample incorporating extra temperature points at low and high temperature. The extended frequency range at 300K shows the TO_2 and TO_4 phonon modes. Data from Fig. 3a are also included for comparison.*

	Sr	Ti	Oxy	Ozx	Oyz
X	0	0.5	0.5	0.5	0
Y	0	0.5	0.5	0	0.5
Z	0.00987045	0.51190984	0.9970011	0.4956093	0.4956093

Table S1 Unit Cell Relative Coordinates from DFT. *Lattice is tetragonal with a_0 = 3.89000 Å and c_0 = 3.91043 Å.*

	Sr	Ti	Oxy	Ozx	Oyz
X	0.02963898	0.04544241	-0.08189972	-0.09030182	-0.07348941
Y	-0.02957567	-0.04530107	0.08204853	0.07359076	0.09041028
Z	0	0	0	0	0

Table S2 Eigenvector for Q_1 mode. *Eigenvector calculated with E_{THz} parallel to (X, -Y, 0). The units of the eigenvector are Å*AMU$^{1/2}$. The eigenvector is normalized so that $\sum \xi_{ijk}^2 m_{jk} = 1$. Here ξ_{ijk} and m_{jk} are the eigenvector and ion mass in AMU, and the indices i,j,k label the eigenvector mode, ion, and coordinate direction.*

	Sr	Ti	Oxy	Ozx	Oyz
X	-0.04831474	0.07770832	0.01575631	0.00874036	0.00874793
Y	0.04829799	-0.07773579	-0.01568512	-0.00870886	-0.00868356
Z	0	0	0	0	0

Table S3 Eigenvector for Q_2 mode. *Eigenvector calculated with E_{THz} parallel to (X, -Y, 0). The units of the eigenvector are Å*AMU$^{1/2}$. The eigenvector is normalized so that $\sum \xi_{ijk}^2 m_{jk} = 1$. Here ξ_{ijk} and m_{jk} are the eigenvector and ion mass in AMU, and the indices i,j,k label the eigenvector mode, ion, and coordinate direction.*

$\omega_1/(2\pi)$	1.669 THz	κ_1	8900 THz^{2}Å^{-2}AMU^{-1}	χ	4000 THz^{2}Å^{-2}AMU^{-1}
$\omega_2/(2\pi)$	5.186 THz	κ_2	**1066 THz^{2}Å^{-2}AMU^{-1}**	ψ_{12}	-4000 THz^{2}Å^{-2}AMU^{-1}
$\gamma_1/(2\pi)$	0.900 THz	Z_1^*	**2.6 e$^-$AMU$^{-1/2}$**	ψ_{21}	**-841 THz^{2}Å^{-2}AMU^{-1}**
$\gamma_2/(2\pi)$	0.150 THz	Z_2^*	**0.2 e$^-$AMU$^{-1/2}$**	β	0.215

Table S4 Model parameters. *Values in bold are unmodified from DFT calculations at 0 K. Values in red were extracted from spectroscopy and literature. Parameters κ_1, ψ_{12}, and χ were initially established by DFT and then tuned to best fit the experimental data. The parameter β was informed by calculations for the expected field screening inside the STO film on the LSAT substrate but was fine-tuned to best fit the experimental data. The linewidth γ_2 was estimated from the trXRD data in the frequency domain.*

Comments on Mode Symmetry in STO Film

In bulk STO, there are four sets of optical phonons, with symmetries (in order of increasing frequency) T_{1u}, T_{1u}, T_{2u}, and T_{1u} [S1]. The three T_{1u} modes are all IR active and in addition possess LO/TO splitting. The T_{2u} mode is known as "silent" because it lacks both IR and Raman activity [S2]. This mode lacks TO/LO splitting. The mode frequencies at 85K are presented in Table S5 and labeled according to [S3].

Mode	Frequency (cm^{-1})	Frequency (THz)
TO_1 (soft)	31	0.93
LO_1	170.6	5.114
TO_2	172.5	5.171
T_{2u} (TO_3, LO_2) (silent)	265	7.94
LO_3	469.5	14.08
TO_4	544	16.3
LO_4	801	24.0

Table S5 Bulk STO Mode Frequencies at 85 K. *Values are extracted from Barker [S3].*

In our film, however, the substrate is compressive and makes the STO film slightly tetragonal (see static x-ray characterization in Figure S2). This changes the space group to *P*4*mm* and the point group at zone center to 4*mm* (C_{4v}). Therefore this alters the symmetries of the four modes according to the rules: $T_{1u} \rightarrow A_1 + E$, $T_{2u} \rightarrow B_1 + E$. The A_1 and B_1 modes consist of displacements along the cross-plane component, while the E modes consist of displacements in-plane. This splitting should also adjust the frequencies of the modes.

The incident THz field resonantly couples to a near-zone center transverse optical mode (the soft mode) with displacement along the THz polarization direction, [1 -1 0], and with wavevector parallel to the THz wavevector (cross-plane direction). Thus the excited soft mode has displacement vector along [1,-1,0] and wavevector along [0 0 1], and has symmetry E. In addition to observing this feature in our trXRD signal, we also detect oscillations at 5.15 THz and 7.6 THz, close in frequency to the LO_1/TO_2 and T_{2u} (silent) modes in bulk STO.

By symmetry, we can only couple the E-symmetry soft mode to other modes of symmetry E by a fourth-order coupling term (e.g. $Q_1^2Q_2^2$ or $Q_1^3Q_2$). Additionally, our x-ray scattering geometry is only sensitive to motion with some component parallel to the x-ray scattering vector, along [2 -2 3]. In-plane, this corresponds to the [1 -1 0] direction.

Thus, while we can couple to E modes with polarization along [1 1 0] we cannot detect them with our choice of x-ray scattering geometry. Our x-ray scattering geometry is also sensitive to displacements in the cross-plane direction [0 0 1] however these modes are symmetry A_1 and therefore require a different coupling term. Specifically, at lowest order we would have either $Q_1^2Q_2$ and then $Q_1^4Q_2$. These features would manifest respectively as signal at $2 * \omega_1/2\pi$ (3.3 THz) and $4 * \omega_1/2\pi$ (6.7 THz) which we do not observe.

Hence we attribute the oscillatory components at 5.15 and 7.6 THz in our x-ray scattering signal to transverse optical phonons with symmetry E with displacements along [1 -1 0]

and wavevectors along [0 0 1]. We then label these three coupled modes as TO_1, TO_2, and TO_3 in order of increasing frequency. Note that from our numerical calculations of the nonlinear phonon coupling terms, we find that T_{1u}(soft) → T_{2u}(silent) coupling while possible is much weaker than E(soft)→E(silent).

References:

S1. Cowley, R. A. Lattice Dynamics and Phase Transitions of Strontium Titanate. *Phys. Rev.* **134**, A981–A997 (1964).

S2. Denisov, V. N., Mavrin, B. N., Podobedov, V. B. & Scott, J. F. Hyper-Raman Spectra and Frequency Dependence of Soft Mode Damping in SrTiO3. *J. Raman Spectrosc.* **14**, 276–283 (1983).

S3. Barker, A. S. Temperature dependence of the transverse and longitudinal optic mode frequencies and charges in SrTiO3 and BaTiO3. *Phys. Rev.* **145**, 391–399 (1966).